VISUALIZATION AND STUDY OF DYNAMIC 2D SHAPES VIA CURVATURE *

SHIN YOSHIZAWA
Graduate School of Computer Science and Engineering
The University of Aizu, Aizu-Wakamatsu shi, Fukushima ken 965-8580 Japan
Phone: 070-5097-5818 Fax: 0242-37-2747 E-mail: m5031126@u-aizu.ac.jp

ALEXANDER BELYAEV
Department of Computer Software
The University of Aizu, Aizu-Wakamatsu shi, Fukushima ken 965-8580 Japan
Phone: 0242-37-2771 Fax: 0242-37-2747 E-mail: belyaev@u-aizu.ac.jp

The paper presents a new result on dynamical properties of the skeleton (medial axis) of a 2D/3D shape and a Java program for visualization, description, and study of dynamic 2D shapes via curvature. The program was developed by the first author and was used by the second author as an education tool for a number of courses (Applied Differential Geometry, Computational Geometry, Mathematical Methods in Computer Graphics) taught at the University of Aizu.

The paper consists of two main sections. A rough description of the program and demonstration of its basic visualization capabilities is provided in the first section. The second section presents a new mathematical result describing dynamical properties of the skeleton (medial axis) of a 2D/3D bounded figure. The 2D version of the result was discovered during authors' experiments with the program.

Topics & Areas: Education and Applications of Multimedia, Topological and Geometric Modeling.

Keywords: visualization, dynamic curves, curvature descriptors, skeleton.

Introduction

Curvature is one of the central concept in the mathematical theory of shape [11], [10]. Being one of the most important intrinsic characteristics of shape, curvature measures deviation from flatness. Visualization and study of curvature-based shape characteristics are very important for shape understanding purposes. The previous research in this field has been mostly concentrated on visualization and analysis of curvature-based characteristics of static shapes.

*The Java applet described in the paper is available at
http://www.u-aizu.ac.jp/~m5031126/Research/CCurve/CCurve.html

In this paper we study and visualize curvature-based characteristics of dynamic shapes.

In the next section we outline the basic capabilities of a Java program for visualization, description, and study of dynamic 2D shapes via curvature. The program was developed by the first author and was used by the second author as an education tool for a number of courses (Applied Differential Geometry, Computational Geometry, Mathematical Methods in Computer Graphics) taught at the University of Aizu.

Next we present a new mathematical result describing dynamical properties of the skeleton (medial axis) of a family of 2D/3D figures. The 2D version of the result was discovered during authors' experiments with the program.

Description and Visualization Capabilities of Program

Basic Options

The program is initialized by displaying a closed quintic B-spline curve, see Fig. 1. A user can modify the shape of the curve by dragging control points,

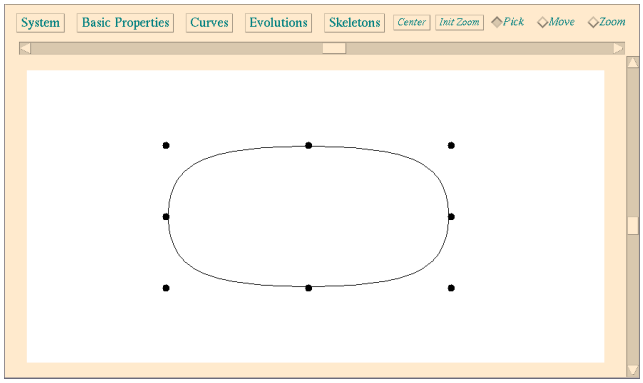

Fig. 1. Java 2D Dynamic Curve Simulator

see Fig. 2. The main window has five main control buttons. Clicking a button opens a subwindow (panel) allowing a user to visualize certain geometric features associated with the curve. Fig. 3 shows the System and Basic Properties panels.

Clicking the Clear Memory button initializes the program, pushing the Split Control Points button increases the number of control points to six-

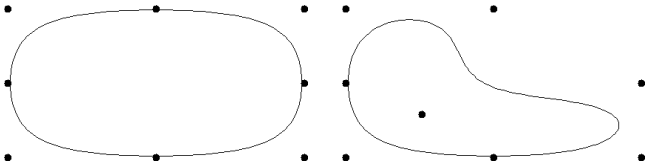

Fig. 2. Left: An initial closed B-spline curve and its control points. Right: A curve obtained by dragging one control point.

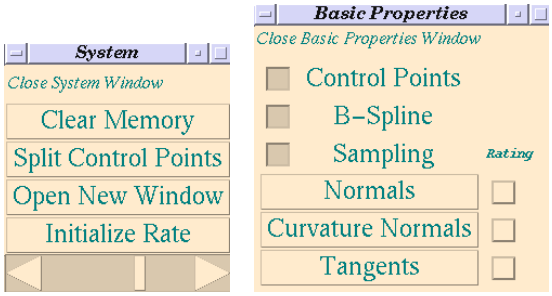

Fig. 3. The SYSTEM and BASIC PROPERTIES panels.

teen, and clicking the OPEN NEW WINDOW button opens a new basic window shown at Fig. 1.

Many implemented algorithms are based on a polygonal interpolation of the basic B-spline curve. The horizontal slider at the bottom of SYSTEM panel allows a user to change the sampling rate of the implemented polygonal interpolation. Clicking the button INITIALIZE RATE sets the finest available polygonal interpolation.

Using the BASIC PROPERTIES panel a user can visualize tangent, normal, and curvature vectors of the curve, see Fig. 4.

The checkboxes CONTROL POINTS, B-SPLINE, and SAMPLING visualize / hidden the control points, the curve, and the interpolating polygon, respectively. The checkboxes RATING allow a user display normals, curvature normals, and tangents at the interpolation points only. Visualizing the curvature vectors (curvature profile) is often used for shape quality evaluation properties [8].

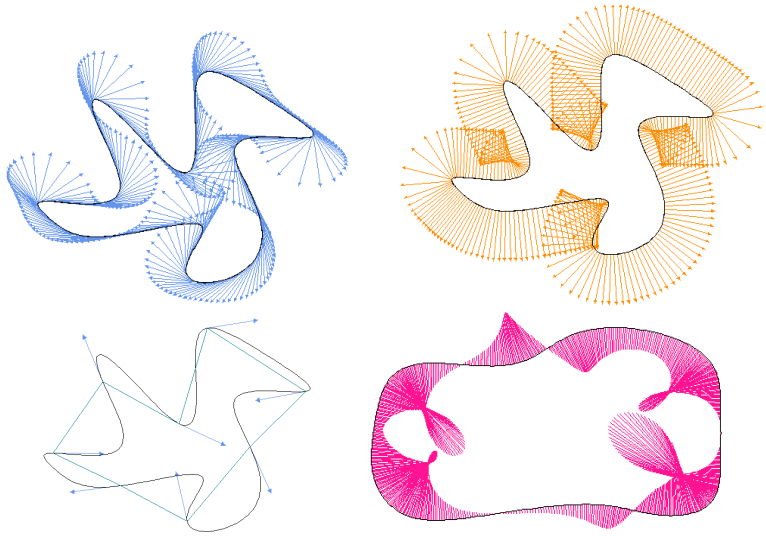

Fig. 4. Top-left: a curve and its unit tangent vectors. Top-right: a curve and its outer normals. Bottom-left: the effect of the RATING checkbox associated with the TANGENTS button is demonstrated, only the tangent vectors at the interpolating points are displayed. Bottom-right: a curve and its curvature vectors; such curvature profile is often used for shape quality evaluation properties.

Evolute, Offsets, and Caustics by Reflection.

The CURVES panel, see Fig. 5, allows a user to visualize the osculating circles, evolute, offset curves, and caustics by reflection associated with of the main B-spline curve.

Evolute and offset curves. Let us recall that the best approximation of a curve at its point P by a circle is given by the *circle of curvature* called also the *osculating circle* at P [15]. If P is an inflection point (where the curvature is zero), the circle of curvature degenerates into the tangent line at P.

The locus of the centers of curvature of a given curve is called the *evolute* of the curve. The evolute of a smooth curve has singularities (so-called cusps). As we will see in the second section of the paper, the singularities of the evolute correspond to the points where the curvature takes extremal values.

An *offset curve* is the locus of points equidistant from a given curve. Offset curves have numerous applications in manufacturing [8,9]. The offset curves also may have singularities. The singularities of the offset curves are

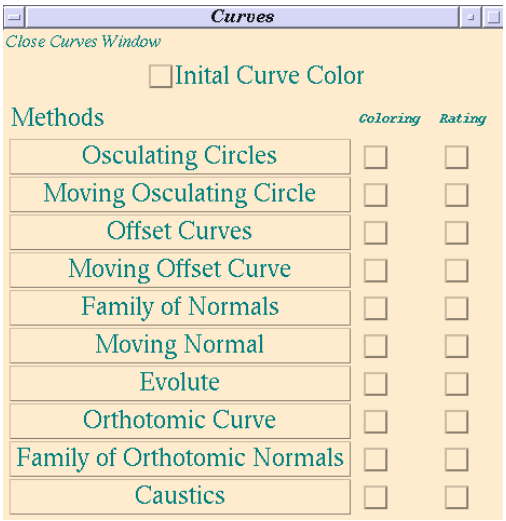

Fig. 5. The CURVES panel.

situated on the evolute.

The Java 2D Curve Simulator allows to visualize many interesting properties of the evolute, osculating circles, and offset curves. See Fig. 6.

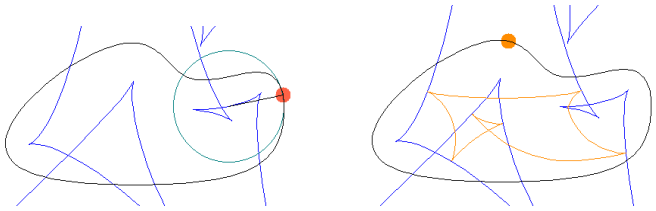

Fig. 6. Left: A curve, its evolute, and an osculating circle; note that the segment connecting the circle center and the tangency point is tangent to the evolute. Right: The same curve, its evolute, and an offset curve; note that the cusps of the offset curve are situated on the evolute.

A user can drag the tangency point and move the osculating circle along the curve. Similar control capabilities are provided for the offset curves.

The evolute can be also described as the envelope of the curve normals. Clicking the FAMILY OF NORMALS button (see Fig. 5) allows to visualize this

optical property of the evolute.

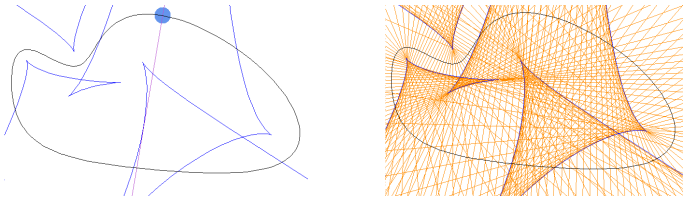

Fig. 7. Left: a curve, its evolute, and a normal. Right: the evolute is given as the envelope of all the normals.

Caustic by reflection, orthotomic. The envelope of the family of straight lines is called a *caustic*. For example, a so-called coffeecup caustic is formed by sun rays reflected by the inner surface of a cup when the sun shines on it.

Consider a point O and a curve not passing through O. The locus of the reflections of O with respect to all the tangent lines to the curve is called the *orthotomic* of the curve relative to O, see Fig. 8.

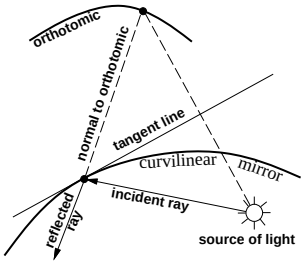

Fig. 8. The orthotomic is formed by the reflections of a given source of light with respect to all the tangent lines.

Imagine that a point source of light is located at O. and light from O is reflected from the curve according to the usual rule that the reflected ray and the incident ray make equal angles on opposite sides of the normal of the curve. Then the caustic generated by the reflected rays, the caustic by reflection, is the evolute of the orthotomic [7].

Clicking the Orthotomic Curve, Family of Orthotomic Normals, and Caustics buttons (see Fig. 5) visualize the orthotomic, the family of the orthotomic normals, and the caustic by reflection, respectively. A user can also

drag the source of light point by mouse and study dynamical properties of the orthotomic and caustic by reflection.

The top-left image of Fig. 9 exposes the coffeecup caustic, the top-right and bottom-left images explain how the coffeecup caustic is modeled, and and the bottom-right image shows the associated orthotomic curve.

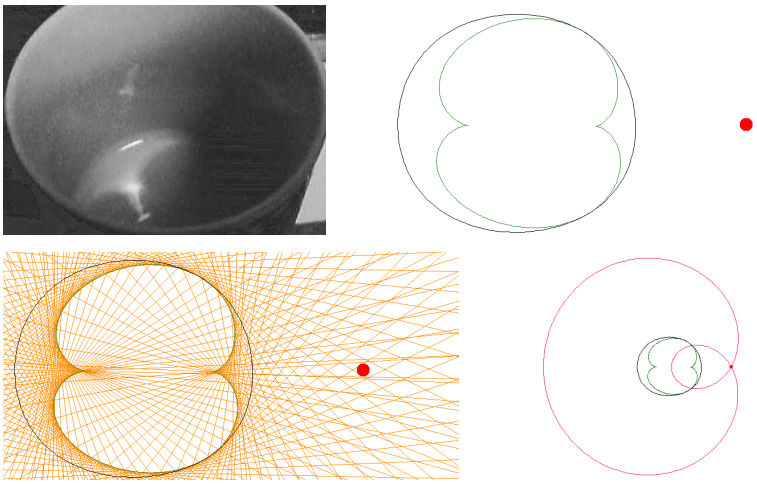

Fig. 9. Coffeecup caustic.

Playing with the caustic by reflection, one can observe, for example, the following delicate result [7]: the caustic is always tangent to the curve at the points where the light rays emitted from the source are tangent to the curve.

Curve Evolutions

Let us consider a family of simple closed smooth curves $\mathcal{C}(p,t)$, where p parameterizes the curve and t parameterizes the family. Assume that p is independent of t.

Let us assume that this family evolves according to the evolution equation

$$\frac{\partial \mathcal{C}(p,t)}{\partial t} = F(k)\,\mathbf{n}, \qquad \mathcal{C}(p,0) = \mathcal{C}^{(0)}(p), \tag{1}$$

where $\mathbf{n}(p,t)$ is the unit normal vector for $\mathcal{C}(p,t)$, F is the evolution speed given as a function of the curvature k. The family parameter t can be considered as the time duration of the evolution.

The study of families of plane curves evolving according to (1) has recently been a subject of intensive research (see, for instance, [13] and references therein) in connection with multiscale shape analysis and geometrical image processing.

The following four curve evolutions are implemented in the program:

- (1) with $F \equiv k$ (the so-called *curve shortening flow*);
- (1) with $F \equiv c + d \cdot k$, where c and d are constants;
- (1) with $F \equiv -1$ (the *distance-function flow*, the evolving curve generates level sets of the distance function from the initial curve $\mathcal{C}(p, 0)$);
- the Laplacian flow (a discrete approximation for the curve shortening flow).

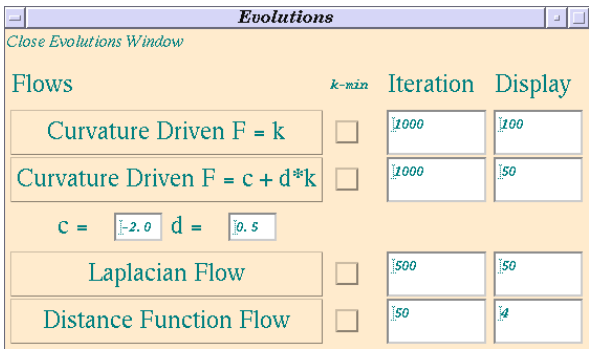

Fig. 10. The EVOLUTIONS panel.

Numerical implementation of the flows combines the forward Euler scheme for (1) and polygonal approximation for the evolving curve $\mathcal{C}(p, t)$ (for a detail explanation of the implemented numerical method, see [2]).

The EVOLUTIONS panel, see Fig. 10, allows a user to visualize the above four evolutions. Fig. 11 demonstrates the above evolutions.

Besides, by clicking the K-MIN checkboxes, a user can trace curvature extrema (the curvature negative minima for a curve oriented by its outer normal) and singularities of a curve evolving by one of the four above flows. For example, Fig. 12 demonstrates evolution of curvature extrema and singularities of a curve driven by the curve shortening flow (left) and the distance-function flow (right).

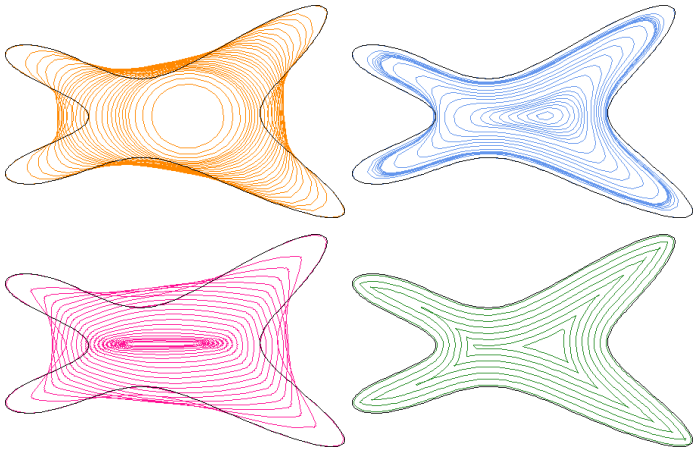

Fig. 11. Top-left: the curve shortening flow. Top-right: the modified curve shortening flow. Bottom-left: the Laplacian flow. Bottom-right: the distance-function flow.

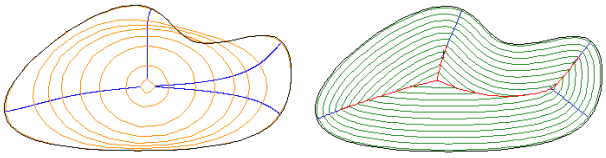

Fig. 12. Left: curvature extrema of a curve evolving according to the curve shortening flow are traced. Right: curvature extrema and singularities of a curve evolving according to the distance-function flow are traced.

Skeleton

The *skeleton* or *medial axis* of a figure F is the closure of the set of points inside F that have more than one closest point among the points of ∂F.

The skeleton is an important shape descriptor invented by Blum [6]. It is extensively used in connection with human shape perception theories [5], [11]. See Fig. 13 for a closed curve and its skeleton. The SKELETON panel is exposed in Fig. 14.

For a 2D simple closed curve, the skeleton can also be defined as the locus of centers of inner circles that are bitangent to the curve. Clicking the SKELETON VIA BITANGENT CIRCLE, MOVING BITANGENT CIRCLE, BITANGENT CIRCLE buttons generates the skeleton of a curve, an inner bitangent circle

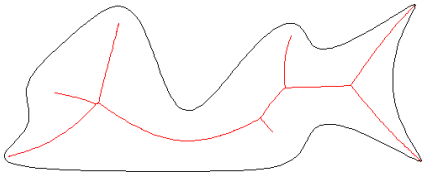

Fig. 13. A closed curve and its skeleton.

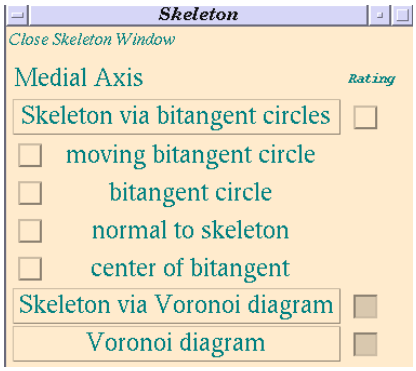

Fig. 14. The SKELETON panel.

which can be dragged along the curve, and a family of inner bitangent circles, respectively.

The notion of the skeleton is closely related to the notion of the Voronoi diagram of a set of points. A numerical method to construct the skeleton from the Voronoi diagram of interpolating polygon is implemented. The method is activated via the buttons SKELETON VIA VORONOI DIAGRAM and VORONOI DIAGRAM.

Fig. 15 shows both the methods to reconstruct the skeleton of a 2D figure.

A user can change the sampling rate of the polygonal interpolation via the horizontal slider of the SYSTEM panel. Fig.16 demonstrates how the approximation of the skeleton via a subset of the Voronoi diagram of the interpolating polygon depends on the sampling rate of the polygonal interpolation.

Skeleton Branching Theorem

In this section we prove the following result describing dynamic properties of the skeleton (medial axis) of a 2D figure. Consider an evolving simple closed curve oriented by its inner normal, a figure bounded by the curve and the medial axis (skeleton) of the figure. A new segment of the medial axis appears / disappears when an evolute cusp corresponding to a positive maximum of the curvature intersects the medial axis. A similar result is obtained for 3D figures.

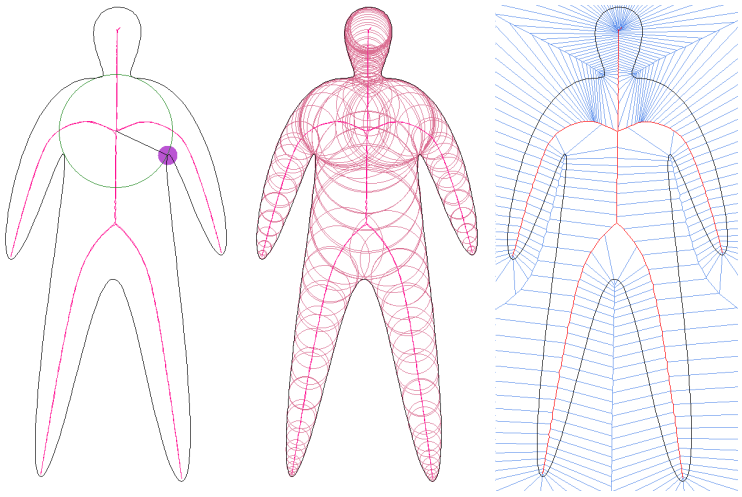

Fig. 15. Left: a figure, its skeleton, and an inner bitangent circle. Middle: the skeleton as the locus of centers of all inner bitangent circles. Right: the skeleton approximated by a subset of the Voronoi diagram of a dense set of points located on the boundary of the figure.

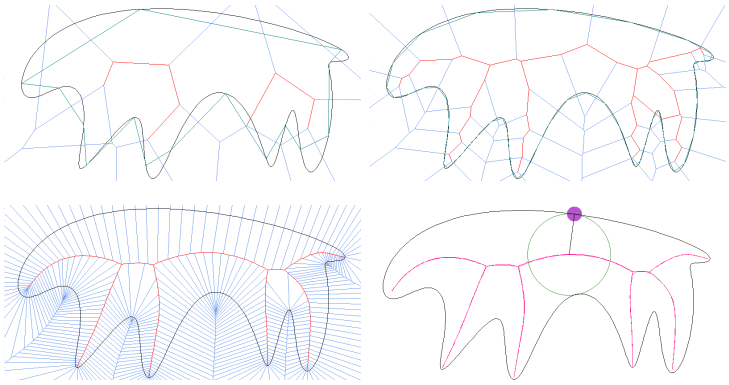

Fig. 16. Top-left: the approximation of the skeleton via a subset of the Voronoi diagram of a sparse set of boundary points. Top-right: the approximation of the skeleton with a denser set of boundary points. Bottom-left: a sufficiently dense set of boundary points leads to a good approximation of the skeleton. Bottom-right: the skeleton as the locus of centers of inner bitangent circles.

2D Skeleton Branching Theorem

Consider a family of simple closed curves. The following theorem describes the evolution of the skeletons of the figures bounded by the curves.

2D Skeleton Branching Theorem: For an evolving simple closed curve, consider the motion of an evolute cusp which lies inside the curve and points towards the curve (i.e., corresponds to a positive maximum of the curvature, if the curve is oriented by its inner normal). When the cusp intersects the skeleton, a new branch of the skeleton is born with its end-point at the cusp.

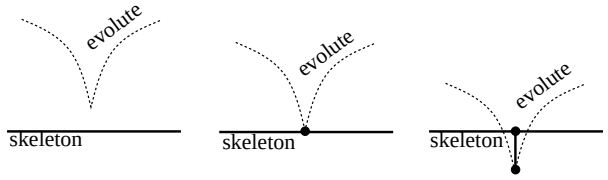

Fig. 17 below provides with a visualization of the 2D Skeleton Branching Theorem.

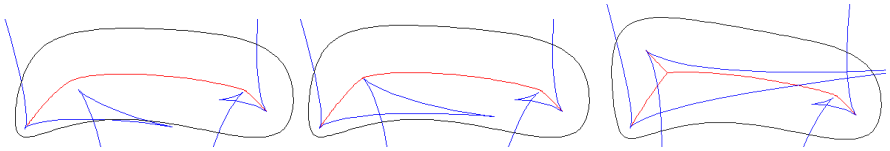

Fig. 17. From top to bottom: a cusp of the evolute intersects the skeleton and a new branch of skeleton is born.

Before proving the theorem, we have to study properties of the evolute and skeleton in more detail.

Evolute. Let us consider a curve $\mathbf{r} = \mathbf{r}(s)$ parameterized by arc length s. To study the shape of the evolute at a small vicinity of a point $\mathbf{r}(s)$ we expand $\mathbf{r}(s+\alpha)$ into Taylor series with respect to α, $\alpha \ll 1$. Let

$$\mathbf{r}' = \mathbf{t} \quad \text{and} \quad \mathbf{n} = \mathbf{t}^{\perp}$$

compose the Frenet frame at $\mathbf{r} = \mathbf{r}(s)$. The evolute is given by

$$\mathbf{e}(s) = \mathbf{r}(s) + \frac{\mathbf{n}(s)}{k(s)},$$

where $k(s)$ is the curvature of the curve at $\mathbf{r}(s)$. According to the Frenet formulas

$$\mathbf{t}' = k\,\mathbf{n}, \quad \mathbf{n}' = -k\,\mathbf{t}$$

we have

$$\mathbf{r}' = \mathbf{t}, \qquad \mathbf{r}'' = \mathbf{t}' = k\,\mathbf{n}, \qquad \mathbf{r}''' = (k\mathbf{n})' = k'\mathbf{n} - k^2\mathbf{t}.$$

It yields

$$\begin{aligned}\mathbf{r}(s+\alpha) &= \mathbf{r} + \alpha\mathbf{r}' + \frac{\alpha^2}{2}\mathbf{r}'' + \frac{\alpha^3}{6}\mathbf{r}''' + O\left(\alpha^4\right) = \\ &= \mathbf{r}(s) + \mathbf{t}\left[\alpha - \frac{\alpha^3}{6}k^2 + O\left(\alpha^4\right)\right] + \mathbf{n}\left[\frac{\alpha^2}{2}k + \frac{\alpha^3}{6}k' + O\left(\alpha^4\right)\right].\end{aligned}$$

Similarly,

$$\mathbf{n}' = -k\mathbf{t}, \quad \mathbf{n}'' = (-k\mathbf{t})' = -k'\mathbf{t} - k^2\mathbf{n}, \quad \mathbf{n}''' = (-k'' + k^3)\,\mathbf{t} - 3k'k\,\mathbf{n},$$

$$\begin{aligned}\mathbf{n}(s+\alpha) = \mathbf{n}(s) + \mathbf{t}\left[-\alpha\,k - \frac{\alpha^2}{2}k' + \frac{\alpha^3}{6}\left(k^3 - k''\right) + O(\alpha^4)\right] + \\ + \mathbf{n}\left[-\frac{\alpha^2}{2}k^2 - \frac{\alpha^3}{2}kk' + O(\alpha^4)\right],\end{aligned}$$

$$k(s+\alpha) = k(s) + \alpha\,k' + \frac{\alpha^2}{2}k'' + O(\alpha^3),$$

$$\frac{1}{k(s+\alpha)} = \frac{1}{k(s)} - \alpha\,\frac{k'}{k^2} + \alpha^2\left(\frac{k'^{\,2}}{k^3} - \frac{k''}{2k^2}\right) + O(\alpha^3).$$

For the evolute point $\mathbf{e}(s+\alpha)$ we have

$$\mathbf{e}(s+\alpha) = \mathbf{r}(s+\alpha) + \frac{\mathbf{n}(s+\alpha)}{k(s+\alpha)} = \mathbf{e}(s) + \tag{2}$$

$$+\,\mathbf{t}\left[\alpha^2\frac{k'}{2k} + \alpha^3\left(\frac{k''}{3k} - \frac{k'^{\,2}}{2k^2}\right) + O(\alpha^4)\right] \tag{3}$$

$$+\,\mathbf{n}\left[-\alpha\,\frac{k'}{k^2} + \alpha^2\left(\frac{k'^{\,2}}{k^3} - \frac{k''}{2k^2}\right) + O(\alpha^3)\right]$$

Thus, if $k'(s) \neq 0$, in a small vicinity of the center of curvature $\mathbf{r}(s)+\mathbf{n}(s)/k(s)$ the evolute is approximated by a parabola tangent to the normal $\mathbf{n}(s)$ (see the left image of Fig. 18). If $k'(s) = 0$, in a small vicinity of the center of curvature

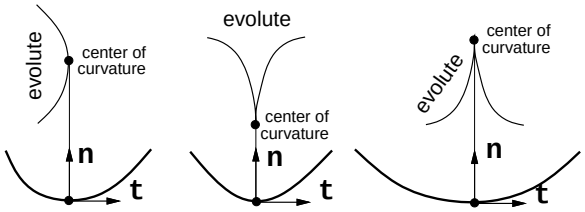

Fig. 18.

the evolute is approximated by a semicubic parabola $y^3 = Ax^2$ tangent to the normal $\mathbf{n}(s)$ (see the middle and right images of Fig. 18).
Thus the evolute is tangent to the curve normals at the centers of curvature.

If $k' > 0$, the vectors $\mathbf{t_e} = \mathbf{n}$ and $\mathbf{n_e} = -\mathbf{t}$ form the Frenet basis of the evolute and reparameterization of (2) gives

$$\mathbf{e}(s+\alpha) = \mathbf{e}(s) + \mathbf{t_e}\left[\beta + O(\beta^2)\right] + \mathbf{n_e}\left[\frac{\beta^2}{2}\frac{k^3}{k'} + O(\beta^3)\right],$$

where $\beta = \alpha k'/k^2$. Thus the curvature of the evolute is k^3/k' and the evolute has no inflections.

A *vertex* of a smooth curve is a point of the curve where the curvature takes an extremal value. A little bit more detail analysis of (2) leads us to the following result (see also [12])

Proposition 1 *The evolute of a curve* $\mathbf{r}(t)$ *has a cusp at* t_0 *if and only if* $\mathbf{r}(t_0)$ *is a vertex of the curve. The cusp on the evolute is pointing towards or away from the vertex according as the absolute value of the curvature has a local minimum or maximum at* t_0.

For a generic curve, the osculating circles centered at ordinary evolute points intersect the curve. The osculating circles centered at the cusps of the evolute have either inner or outer contacts with the curve.

Skeleton. The circle of curvature centered at a skeleton end-point can be considered as a limit of the inner bitanget circles whose centers form the skeleton. Thus the circle is osculating and it has an inner contact with the boundary of the figure. If the boundary of the figure is oriented by its inner normal, the end-points of the skeleton correspond to positive maxima of the curvature of the boundary. Taking into account (2) we obtain the following result.

Proposition 2 *The end-points of the skeleton of a figure are located at cusps of the evolute of the boundary of the figure. Those cusps are pointing towards the boundary of the figure.*

For a simple closed curve, the evolute cusps do not necessary coincide with the end-points of the skeleton of the figure bounded by the curve. If the osculating circle centered at a cusp of the evolute does not lie inside the figure, then the cusp is not a skeleton end-point.

Now the proof of the 2D skeleton branching theorem can be easily derived from the following simple observation: when the cusp intersects the skeleton, the osculating circle centered at the cusp becomes also an inner bitanget circle.

3D Skeleton Branching Theorem

Focal surface. Consider a smooth generic surface. Denote by $k_{\max}$ and $k_{\min}$ the largest and the smallest principal curvatures, respectively, $k_{\max} \geq k_{\min}$. The principal centers of curvature are the points situated on the surface normals at the distances $1/k_{\max}$ and $1/k_{\min}$ from the surface. The loci of the principal centers from the focal surface. The focal surface consists of two sheets corresponding to the maximal and minimal principal curvatures.

The focal surface is the 3D analog of the evolute and has singularities. The singularities of the focal surface consists of space curves called the *focal ribs*. Near a point of a focal rib the focal surface can be locally represented in the parametric form $(c_1 t^3, c_2 t^2, s)$, where $c_1 \neq 0 \neq c_2$, in proper coordinates (s, t). See Fig. 19 for a typical focal rib. The focal ribs themselves have singularities.

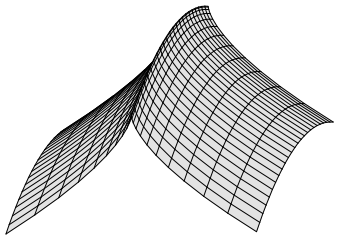

Fig. 19. A typical focal rib.

The surface curves corresponding to the focal ribs are natural generalization of the curve vertices for surfaces.

For a surface given parametrically $\mathbf{r} : \mathbf{R}^2 \to \mathbf{R}^3$, its focal surface is described by:

$$\mathbf{f}(u,v) = \mathbf{r}(u,v) + \frac{\mathbf{n}(u,v)}{k(u,v)}, \qquad k = k_{\max},\, k_{\min}, \tag{4}$$

where $\mathbf{n}(u,v)$ is the oriented normal (without loss of generality we do not consider parabolic points in (4)).

Let at a point P on the surface the coordinates u, v be chosen so that the tangent vectors $\partial\mathbf{r}/\partial u$ and $\partial\mathbf{r}/\partial v$ coincide with the principal directions $\mathbf{t}_{\max}$

and $\mathbf{t}_{\min}$. If P corresponds to a singular point on the focal surface, then the cross product

$$\frac{\partial \mathbf{f}}{\partial u} \times \frac{\partial \mathbf{f}}{\partial v} = \frac{\partial \mathbf{r}}{\partial u} \cdot \frac{\partial k}{\partial u} \cdot \frac{k - k_{\min}}{k^3} + \frac{\partial \mathbf{r}}{\partial v} \cdot \frac{\partial k}{\partial v} \cdot \frac{k - k_{\max}}{k^3}$$

vanishes for where $k = k_{\max}$ and $k = k_{\min}$. This proves the following statement.

Proposition 3 *For a smooth generic surface the singularities of the focal surface (focal ribs) correspond to the lines on the surface where the principal curvatures have extrema along their associated principal directions and the points where the principal curvatures are equal (umbilics).*

Following [8] let us call the surface curves corresponding to the focal ribs by the *principal curvature extremum curves.*

Skeleton. The skeleton (medial axis) of a 3D figure F is the closure of the set of points inside F that have more than one closest point among the points of ∂F.

One can define the skeleton of F as the locus of centers of maximal balls: balls inside F that are not themselves enclosed in any other ball inside F.

Various elements of the skeleton of a figure are schematically shown in Fig. 20 (we use the terminology accepted in [14] and [16]).

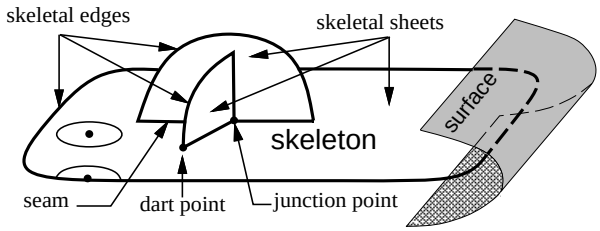

Fig. 20.

The *skeletal edge* of the skeleton of a figure is a connected space curve consisting of the skeletal points whose small neighborhoods on the skeleton are topologically equivalent to a half-disk. One can also describe the skeletal edge points as the points whose maximal spheres have a single contact with the surface bounding the figure. A *skeletal sheet* is a connected component of the skeletal points whose small neighborhoods on the skeleton are topologically equivalent to a disk. A *dart point* is a skeletal point whose small neighborhood on the skeleton is topologically equivalent to a disc sewn with a quarter-disk.

A *junction point* is a skeletal point whose small neighborhood on the skeleton is topologically equivalent to a disc sewn with three quarter-disks. See Fig. 20.

For a smooth oriented surface, let us define the *ridges* as the loci of the positive maxima of the maximal principal curvature along its curvature line.

Relations between the skeletal edges, the ridges, and certain focal ribs are described by the following proposition (see [3], [1], and [4]).

Proposition 4 *Consider a bounded 3D figure F whose boundary, ∂F, is smooth and oriented by its inner normal. The skeletal edges are a subset of the focal ribs associated with the maximal principal curvature and pointing towards ∂F. Those ribs correspond to the ridges on ∂F.*

These relations between the ridges, the focal ribs associated with $k_{\max}$ and pointing towards the surface, and the skeletal edges are demonstrated schematically in Fig.21 and for an elliptic paraboloid in Fig. 22.

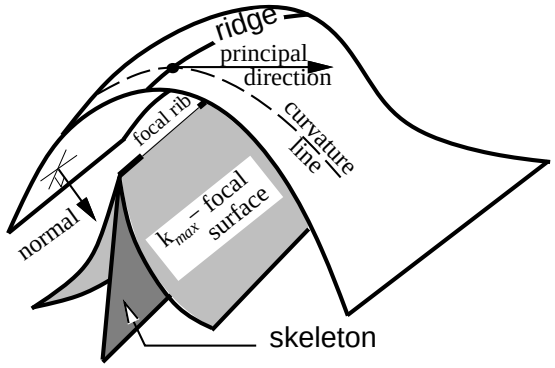

Fig. 21.

A proof of Proposition 4 is sketched in the next three subsections.

Ridges. Consider a smooth surface. For a given non-umbilic point P on the surface let us choose coordinates in the space so that P is at the origin, the (x, y)-plane is the tangent plane to the surface at P, the principal directions $\mathbf{t}_{\max}$ and $\mathbf{t}_{\min}$ coincide with x and y axes, respectively, and the normal $\mathbf{n}$ coincides with z-axis. Then the surface is expressible in the Monge form as the graph of a generic smooth function $z = F(x, y)$, where

$$F(x,y) = \frac{1}{2}\left(\lambda x^2 + \mu y^2\right) + \frac{1}{6}\left(ax^3 + 3bx^2y +\right.$$

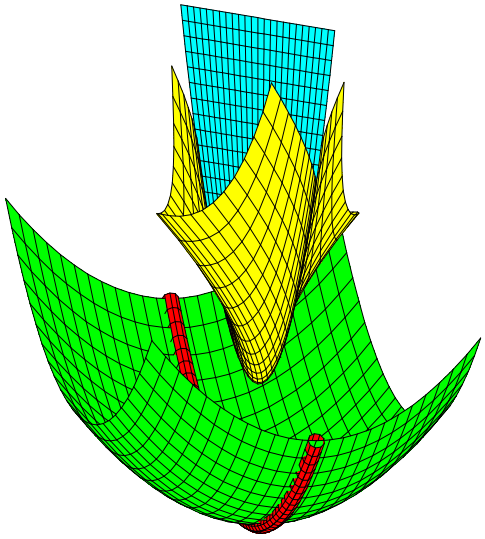

Fig. 22. A surface, a ridge on the surface, the focal surface sheet associated with $k_{\max}$, and the skeleton of the figure bounded by the surface.

$$+ 3cxy^2 + dy^3) + \frac{1}{24}\left(ex^4 + 4fx^3y + \ldots\right) + O(x,y)^5$$

with $\lambda = k_{\max}(0,0)$, $\mu = k_{\min}(0,0)$, $\lambda > \mu$.

The Taylor series expansion of $k_{\max}$ at P has the form

$$k_{\max}(x,y) = \lambda + ax + by + O(x,y)^2.$$

Since the vectors $(1,0)$ and $(0,1)$ represent $\mathbf{t}_{\max}$ and $\mathbf{t}_{\min}$ at P, respectively, then

$$\frac{\partial k_{\max}}{\partial \mathbf{t}_{\max}}(0,0) = a \qquad \frac{\partial k_{\max}}{\partial \mathbf{t}_{\min}}(0,0) = b \tag{5}$$

Let $e_{\max} = \partial k_{\max}/\partial \mathbf{t}_{\max}$. The extrema of the maximal principal curvature along its curvature line are given in the implicit form by the zero-crossings of $e_{\max}$.

Let the surface orientation be chosen so that the maximal principal curvature is strictly positive at P

$$k_{\max}(0,0) > 0.$$

The curvature line associated with $k_{\max}$ is locally described by the problem

$$\frac{dy}{dx} = \frac{bx + cy}{\lambda - \mu} + O(x, y)^2, \qquad y(0) = 0.$$

Therefore, $y'(0) = 0$, $y''(0) = b/(\lambda - \mu)$ and in a neighborhood of the origin the curvature line is approximated by the parabola

$$y = \frac{bx^2}{2(\lambda - \mu)}.$$

It allows to compute the Taylor series expansion of $k_{\max}$ at the origin along the associated curvature line

$$\lambda + ax + \left(-3\lambda^3 + e + \frac{3b^2}{\lambda - \mu}\right)\frac{x^2}{2} + O(x^3) \tag{6}$$

Analyzing asymptotic expansion (6) we obtain that P is a generic ridge point (the maximal principal curvature has a positive maximum along its curvature line) iff

$$\lambda > 0, \quad a = 0, \quad A = -3\lambda^3 + e + \frac{3b^2}{\lambda - \mu} < 0. \tag{7}$$

Note that

$$A = \frac{\partial e_{\max}}{\partial \mathbf{t}_{\max}}(0,0) = \frac{d^2 k_{\max}}{ds_{\max}^2}(0,0),$$

where $s_{\max}$ is the arclength of the curvature line associated with $k_{\max}$.

If P is a ridge point, the tangent direction to the ridge at P is given by $\{Ax + By = 0,\ z = 0\}$, where

$$A = \frac{\partial e_{\max}}{\partial \mathbf{t}_{\max}}(0,0) \quad \text{and} \quad B = \frac{\partial e_{\max}}{\partial \mathbf{t}_{\min}}(0,0) = f + \frac{3bc}{\lambda - \mu}.$$

Contact with osculating spheres. Let us consider the loci of points where the curvature of the intersection curve between the surface and the plane $\{y = \alpha z\}$, where α is a parameter. The intersection curve between the surface and the plane is locally described by the equation $y = \alpha\lambda x^2/2 + \ldots$. The Taylor expansion of the curvature of the curve is the product of $\sqrt{1+\alpha^2}$ and

$$\lambda + ax + \left(-3\lambda^3(1+\alpha)^2) + 3\lambda^2\mu\alpha^2 + 6b\lambda\alpha^2 + e\right)\frac{x^2}{2} + O(x^3) \tag{8}$$

Thus, if the origin is a ridge point ($a = 0$), the type of the extremum of the curvature at the origin is defined by the sign of

$$-3\lambda^3(1+\alpha)^2) + 3\lambda^2\mu\alpha^2 + 6b\lambda\alpha^2 + e.$$

This expression is a quadratic polynomial in α. The discriminant is given by

$$D = 3\lambda^2(\lambda - \mu)A,$$

where A is defined in (7). Now from (6) it follows that the osculating spheres (spheres of curvature) associated with $k_{\max}$ have inner contacts with the surface at the ridge points.

Ridges and Focal Ribs. The intersection between the caustic sheet associated with $k_{\max}$ and the plane $\{y = 0\}$ gives a curve described locally by

$$x = -\frac{A}{3\lambda}t^3 + O(t^4), \quad z = \frac{1}{\lambda} - \frac{A}{2\lambda^2}t^2 + O(t^3).$$

At a neighborhood of the point $(0, 0, 1/\lambda)$ the intersection curve is locally a semicubical parabola. Thus the cuspidal edges (ribs) of the caustic sheet associated with $k_{\max}$ and pointing towards the surface correspond to the ridges.

Skeleton Branching Theorem in 3D. Consider a closed surface and a figure bounded by the surface. The skeletal edges of the skeleton of the figure are not necessary located at focal ribs. If the sphere of curvature (osculating sphere) centered at a focal rib point does not lie inside the figure, then the point is not a skeletal edge point. This observation and the above results on contacts with osculating spheres lead us to the following theorem describing dynamic relations between the skeleton of an evolving figure (i.e., a family of figures) and certain focal ribs of the boundary of the figure.

3D Skeleton Branching Theorem: For an evolving smooth closed surface oriented by its inner normal, consider the motion of a focal rib associated with the maximal principal curvature, situated inside the surface, and pointing towards the surface (i.e., corresponding to a ridge). When the rib intersects the skeleton, a new sheet of the skeleton is born with its skeletal edge located at the rib.

Conclusion

The paper presents a new result on dynamical properties of the skeleton (medial axis) of a 2D/3D shape and a Java program for visualization, description, and study of dynamic 2D shapes via curvature.

References

1. A. G. Belyaev, E. V. Anoshkina, and T. L. Kunii, "Ridges, ravines, and singularities", Chapter 18 in A. T. Fomenko and T. L. Kunii, *Topological Modeling for Visualization*, Springer, 1997.
2. A. G. Belyaev, E. V. Anoshkina, and S. Yoshizawa, and M. Yano, "Polygonal curve evolutions for planar shape modeling and analysis", *International Journal of Shape Modeling*, Vol. 5, No. 2, 1999, pp. 195–217.
3. A. G. Belyaev, I. A. Bogaevski, and T. L. Kunii, "Ridges and ravines on a surface and segmentation of range images", *Vision Geometry VI*, Proc. SPIE 3168, 1997, pp. 106-114.
4. A. G. Belyaev and Yu. Ohtake, "An image processing approach to detection of ridges and ravines on polygonal surfaces", *Eurographics 2000, Short Presentations*, to appear.
5. H. Blum, "A transformation for extracting new descriptors of shape", *Symposium on Models for the Perception of Speech and Visual Form*, MIT Press, 1967, pp. 362–380.
6. H. Blum, "Biological shape and visual science", *J. Theor. Biology*, Vol. 38, 1973, pp. 205–287.
7. J. W. Bruce and P. J. Giblin, *Curves and Singularities : A geometrical introduction to singularity theory*, Cambridge University Press, 1992.
8. M. Hosaka, *Modeling of Curves and Surfaces in CAD/CAM*, Springer, 1997.
9. J. Hoschek and D. Lasser, *Fundamentals of Computer Aided Geometric Design*, A K Peters, 1993.
10. J. J. Koenderink, *Solid Shape*, MIT Press, 1990.
11. D. Mumford, "Mathematical Theories of Shape: Do they model perception?", *Geometric Methods in Computer Vision*, Proc. SPIE 1570, 1991.
12. I. R. Porteous, *Geometric Differentiation for the Intelligence of Curves and Surfaces*, Cambridge University Press, 1994.
13. J. A. Sethian, *Level Set Methods*, Cambridge University Press, 1996.
14. E. C. Sherbrooke, N. M. Patrikalakis, and E. Brisson, "Computation of the medial axis transform of 3-d polyhedra", *Proceedings of the Third Symposium on Solid Modeling and Applications*, 1995, pp. 187–199.
15. D. J. Struik, *Lectures on Classical Differential Geometry*, Dover, 1988.
16. G. M. Turkiyyah, D. W. Storti, M. Ganter, H. Chen, and M. Vimawala, "An acceleration triangulation method for computing the skeletons of free-form solid models", *Computer-Aided Design* Vol. 29, No. 1, 1997, pp. 5–19.